

## **Closure Report (SERB/EMR/2016/008045)**

### **Approved Objectives**

- (i) To probe how definite microstructure/nanostructure based surface roughness becomes responsible for wetting/dewetting response.
- (ii) To evaluate structural colouration by examining surface scattering and sub-surface volume scattering both qualitatively and quantitatively.
- (iii) To establish a bifunctional (dewetting and biophotonic) correlation and consequently, a model knowing that individual properties are based on inbuilt microstructure/roughness.

An in-depth understanding of the structural geometry of the natural systems that dictate both dewetting and colouration characteristics may open up a new avenue for replication in artificial designs and technological assets at large.

### **Deviations made from original objectives (if any)**

The original objectives are generally met with the exceptions that we could not analyse our samples with microspectrophotometry where the typical spot size employed is much smaller (a few tens of  $\mu\text{m}$ ) than that of our case (a few mm). Whereas incident angle-dependent reflectance features and CIE chromaticity diagrams are employed to characterize structural colouration aspects, contact angle measurements with base tilting were considered for evaluating wetting-dewetting characteristics. For colour analysis, 3D scatterograms could not be provided due to a lack of access to specific software. However, incident angle-dependent reflectance, reflectance after chemical treatment, polarization-dependent reflectance etc. have been acquired/analyzed suitably.

Structural colouration is greatly dictated by light scattering events and consequently, reflectance features. The reflectance spectra of the wings, upon ethanol uptake, got altered due to the percolation of ethanol into the built-in microstructure which could influence scattering events substantially. We could not establish a reason conclusively as to why in certain wing types ethanol uptake has improved the reflectance features, while in other cases it offered a reverse trend. On the other hand, the wettability property depends on the water-holding capability on a given surface texture/microstructure. Here, microstructure and surface roughness mediated colouration and wettability features have been encountered in most of the specimens. Though an attempt has been made to offer a quantitative account of contributions due to micro and nanoscale-roughnesses present in the studied specimens, a comprehensive model could not be established. Further, the molecular basis of discolouration effects observed in flower samples after a certain chemical treatment (propanol) could not be attended to.

Bi-functional structural colouration and wettability aspects studied in natural systems have not been translated into artificial material design/structures as they do not constitute part of the main objectives.

### **Concise Research Accomplishment**

Adequate characterization of uni- and multi-colour butterfly wings, as well as rose cultivars, have been performed employing advanced analytical techniques. We began with the uptake of  $\text{Ag}^+$  into scale microstructures of certain butterflies along with consideration of linkage between microstructure make-up and reflectance responses.

-Next, thin-film interference and sub-surface volume scattering which account for whitish structural colouration have been investigated for white admiral, large white and dark blue tiger butterfly wings belonging to the Lepidoptera order. Whereas large white butterfly wings contain adequate pterin pigments, whiteness in other cases is largely characterized by wing surface texture. Also, the large white (LW) and dark blue tiger (DBT) wings are seen to be less polarization-sensitive as compared to their white admiral (WA) wing counterpart.

- The butterfly wings showed truly hydrophobic features (contact angle, CA >90°), but without satisfying the criterion for super-hydrophobicity (CA>140°). While two kinds of surface roughnesses can be anticipated (micro-and nanoscale roughness) in the aforementioned butterflies, the wetting-dewetting aspects have been analysed in conjunction with the different wetting modes, generic (Wenzel, Cassie-Baxter) and vertical gibbosity models.

-In the next round of works, coloured flower petals (*Indian rosacea and Rosa sinensis*) have been considered knowing that floral colouration is the combined result of pigmentary and structural effects. Firstly, structural colouration and discolouration in white (W), light pink (LP) and dark pink (DP) appearing Indian roses were investigated before and after immersion in specific media (methanol, ethanol, propanol and glycerine). Interestingly, after propanol uptake, all these rose petals (W, LP, and DP) gave quite similar reflectance features, possibly due to fading away of colour. Conversely, upon ethanol uptake, the LP and DP rose petals featured similar curves, which may arise due to the sharing of a common micro-texture. With a CA= 133.3°, and a roughness factor of  $r_\phi=2.94$ , the DP petals exhibited the dewetting feature close to super-hydrophobicity. Assuming micro-papillae as regular cylinders, the  $r_\phi$  and solid-water fraction,  $\phi$  could be interlinked suitably. In the second set of studies, structural colouration and dewetting properties of apparent red, pink and yellow hibiscus flowers (*Rosa sinensis*) belonging to the Malvaceae family have been worked out. The specimens are found to be partly polarization-sensitive and that, the pink and yellow petals exhibited relatively higher surface adhesion to water in which the droplets can be pinned to the surface and would not roll off the surfaces, even if the CA>90°.

Three papers [Europhys. Lett. 119, 66003 (2017); J. Bionic Eng. 15, 1012 (2018); Phys. Scr. 96, 085004, (2021)] have been published so far and two manuscripts are still under consideration.

## Experimental/ Theoretical Investigation carried out

(full details of experimental set up, methods adopted, data collected supported by necessary table, charts, diagrams & photographs)

Four major works have been undertaken in the project. Firstly, structural colouration has been exploited in uni- and multi-colour butterfly wings with the consideration of progressive Ag<sup>+</sup> uptake into scale ridges. Secondly, the origin of whitish structural colouration and wettability has been encountered in white admiral (WA), large white (LW) and dark blue tiger (DBT) spotted wings. Next, white (W), light pink (LP) and dark pink (DP) Indian Rosacea specimens were taken for studying structural colouration and discolouration (upon treatment with methanol, ethanol, propanol and glycerine) effects. Lastly, red, pink and yellow hibiscus (*Rosa Sinensis*) flower petals are considered as test samples for assessing structural colouration and wetting-dewetting features.

Specimen collection:

(i) Butterfly specimens- The samples chosen are essentially butterflies locally available in the Indian subcontinent.

As for evaluation, we opted for distinctly different coloured (to the unaided eyes) butterfly species which could account for structural colour contribution. The species collected from our university garden streets are namely, *Papilio Liomedon* (black, 4.5 cm×2.5 cm), *Catopsilia Pyranthe* (faint green, 4.7 cm×2.3 cm) and *Vanessa Cardui* (multi-colour, 4.1 cm× 2.2 cm). The dimensions mentioned are along the length and breadth of a given specimen and measured from tip-to-tip of the wing parts. The wings were gently separated from the main part and then subjected to light air blowing in order to remove the undesired dirt and dust particles out of the wing surfaces. For each species, the central part of the wing has been considered for subsequent experimentation which includes Ag<sup>+</sup> uptake, electron microscopy imaging and reflectance measurements.

In the second round of studies, we considered the white admiral butterfly (WA, *Limenitis Camilla*) of the Nymphalidae family with the wings offering alternate white and brown patches, the large-white butterfly (LW, *Pieris Brassicae*) of the Pieridae family bearing the whole white wings and finally, the dark- blue tiger butterfly (DBT, *Tirumala Septentrionis*) belonging to the Nymphalidae family which offers transparent white-spots embedded in the black wing background. The average tip-to-tip dimensions of these systems are ~64 mm, ~58 mm and ~80 mm; respectively. The butterfly specimens were collected from different locations of the garden street within the ring road of our university campus. The forewings of the WA butterfly were sectioned just after its natural death and the white and brown segments were preserved in separate containers. Similarly, the forewings of the LW and DBT butterflies were collected and sectioned as desired. In order to make them dirt-free, the wing specimens were subjected to mild air blowing prior to further processing and characterization. The sectioned specimens were later dipped in AR-grade ethanol (R.I.=1.36) and left undisturbed overnight.

(ii) Flower specimens-The specimens opted for our work were three varieties of the Rosaceae cultivars, namely, white rose (*Rosa chinensis* var *spontanea*), a light pink rose (*Rosachinensis* var *minima*), and dark pink rose (*Rosa chinensis* var *minima*) and labelled as, W, LP and DP; respectively. To retain the surface property, specimens were generally collected prior to exposure to direct sunlight. Accordingly, fresh flower specimens were gently plucked from our university gardens during morning hours. Moreover, in order to retain the physiological state intact, the time gap between the plucking of flowers and conducting the experiment was kept minimal (< 60 min), for every sample. The average dimension of the petals examined varied in the range of 12 mm – 25 mm. In order to exploit the nature of the discolouration effect each of the specimens was treated with methanol, ethanol, propanol and glycerine separately. In the next set of studies, red, pink and yellow hibiscus (*Rosa sinensis*) flower petals have been collected for subsequent experiments without and with immersion in different media.

#### Methods Adopted:-

In order to exploit microstructural details, a scanning electron microscope (SEM, JEOL-6390LV) has been employed, whereas elemental analysis was performed through the energy-dispersive X-ray spectroscope (EDX, Oxford-7582) attached to the main machine. Micrographs and EDX spectra were captured before and after the Ag<sup>+</sup> uptake process, for every sample (black, green and multi-coloured wings) under study. The room temperature reflectance spectra have been acquired in the wavelength range of 300–800 nm by employing a UV-Vis-NIR spectrophotometer. Emphasis is also given to the study of polarization-sensitive reflectance features, with the help of a linear polaroid that gives p-polarized light. The polaroid and consequently, polar-axis was given a right-handed rotation ( $\theta = 0^\circ, 45^\circ$  and  $90^\circ$ ) about the plane of incidence. In all the cases, however, the normal incidence of light on the sample was considered with the acquired data verified at least three times for the specimens under study.

Similarly, an SEM machine was employed to capture micro-morphological details present in the forewings of WA, LW and DBT butterfly wings. Since the specimens are electrically non-conducting, each of the specimens was coated with a several nm thick Pt layer in order to avoid charging effect during imaging. For analyzing different parts of the micro-structural network, the images were captured at different magnifications (100X, 500X and 10kX) as per requirement. Also two dimensional FFT of 2  $\mu\text{m}$  x 2  $\mu\text{m}$  micrographs have been obtained to examine the spread in spatial frequency of periodic units across position in space.

The reflectance features of the untreated and ethanol-treated specimens were evaluated by employing a UV-Vis-NIR spectrophotometer and acquiring data in the wavelength range of 200–800 nm, with an integrating sphere attached to the main optics while supporting normal incidence. While acquiring reflectance data, the spot size of the beam is kept fixed ( $\sim 2$  mm) and a white reference namely OP.DI.MA (ODM98) has been employed for calibration purpose. In order to ensure the whole reflectance characteristics free from spurious data, we opted for a slow-scanning rate (0.02 nm/s), in each case. First, the reflectance features of the untreated brown and white specimens of the WA butterfly wing were acquired independently. Next, the reflectance data on the white area of the LW butterfly and the spotted-white part of the DBT butterfly wings have been acquired in the same system. For the sake of comparison and further assessment, the reflectance curves of the ethanol-treated specimens were also captured. The alteration of R.I. in the microstructural environment of the ethanol-treated specimens was believed to manifest the overall reflectance of the specimens under study. Also, in order to gain insight as regards, scattering events within the specimens, linear transmittance spectra have been captured for the investigated specimens. Moreover, angle-dependent reflectance characteristics of all the wing-types are obtained on a PerkinElmer machine with variable angle reflectance (VAR) accessories capable of offering incident angle ( $\varphi$ ) variation in the range of 15–75°. Furthermore, series of reflectance data have been acquired by opting s and p- polarized incident light by employing a pair of polaroids sensitive in the range of wavelengths, 400–700 nm. All these experiments were carried out at room temperature (298 K) and without permanent chemical treatment which could alter their chemical composition, or produce byproducts, or even damage their built-in natural microtexture permanently.

The wetting-dewetting features of the specimens were carried out by measuring static water Contact Angles (CA) by employing a contact angle meter (Kyowa Interface Science Co.Ltd.). At first,  $\sim 3$   $\mu\text{L}$  volume droplet of water is gently placed on the petal specimen mounted on the base plate positioned in between the locations of a white light source and CCD camera meant for imaging. The tilting base methodology was also employed to measure the advancing and receding angles and consequently, the Contact Angle Hysteresis (CAH). This forms an important aspect for understanding the wetting-dewetting feature of the given system. The base of the petal surface was subjected to an intermittent tilt mode, and the tilt was varied in the range of  $0^\circ - 90^\circ$ . Measurement of advancing (maximum) and receding (minimum) angles were

repeated at least 10 times for every unit of tilting. The data acquisition was made on a PC equipped with the standard FAMAS software® provided with the machine.

In order to exploit optical features of the flower petals, UV-Vis-NIR reflectance spectroscopy has been employed in the ambient environment. Moreover, in order to evaluate the structural and pigmentary contributions qualitatively, the whole rose and hibiscus petals were treated with different organic media of known refractive indices (RI) viz. ethanol (RI = 1.36), propanol (RI = 1.39) and glycerine (RI = 1.47). Accordingly, the reflectance spectra of the untreated and treated specimens were acquired and analysed. The air gaps and voids to be temporarily filled by these liquids were believed to affect the spectral behaviour immensely over the complete range of wavelengths. Moreover, the floral attributes as revealed from the reflectance spectra were also evaluated with the help of CIE chromaticity diagrams plotted using the CIE 1931 colour space. Wetting-dewetting features were analyzed through static and dynamic CA measurements emphasizing base tilting in the latter case. The CA, CA hysteresis, contact line etc. have been measured for different specimens in order to visualize the role of surface microstructure on surface wettability.

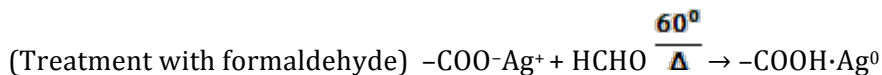
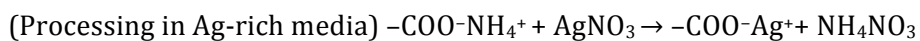
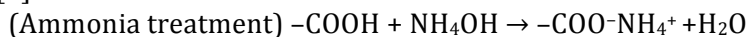
All the experiments were carried out at room temperature. The experimental results were discussed in the light of some theoretical treatment while discussing structural colouration and wettability features.

### Detailed Analysis of result

*(indicating contributions made towards increasing the state of knowledge in the subject)*

#### a) Structural colouration in uni and multi-coloured butterfly wings

Three distinct butterflies namely, *Papilio Liomedon* (black), *Catopsilia Pyranthe* (green) and *Vanessa Cardui* (multi-coloured) were chosen. Each of the ridges in the wing scale was seen to comprise numerous hierarchical microstructures, held precisely through the 2D network. The average width of the strips and ridges varied in the range of 0.15–0.25  $\mu\text{m}$ . The wing makeup comprises alternate chitinous layers decorated with melanin pigments [1] and air-gaps between successive longitudinal ridges running along the length of the scale. The polycyclic macromolecules with their residual  $-\text{COOH}$  groups [2] were believed to provide the desired sites for the  $\text{Ag}^+$  uptake. In the present case, the treatment with a weak alkali (5%  $\text{NH}_4\text{OH}$ ) and subsequent processing in  $\text{AgNO}_3$  has resulted in an adequate reduction of the air gaps with the time duration. The chemical reactions involved for  $\text{Ag}^+$  uptake at the functional sites are given below [3]:



The uptake of  $\text{Ag}^+$  followed by the simultaneous reduction of  $\text{Ag}^+$  into  $\text{Ag}^0$  at the functional sites of the fibrils could yield a cluster of Ag atoms, and eventually a nanosystem. Controlling air-holes along with the growth of Ag nanoparticles in natural templates would form the basis for developing hybrid photonic structures [4]. The infiltration of nanoscale Ag into scales can also be evident from the EDX patterns which displayed a gradual development of the Ag-peak with the processing time. With a variance  $<0.05\%$ , the uptake of  $\text{Ag}^+$  in the butterfly wing scales tending to follow an exponentially growing fit,  $\sim e^{0.36t}$ .

All the specimens showed a high reflectance value above 700 nm. Since the hump at  $\sim 265$  nm characterizes chitin composition [5,6], the spectral analysis was conducted for the wavelength range, 300–800 nm. In the range of 400–650 nm, two distinct features can be found, namely, an abrupt rising trend and a steady growth. It is worth mentioning here that human

eyes are less sensitive to wavelengths that fall below UV and above IR spectra [7]. As for the black specimen, a small, yet uniform reflectance feature (~5%), has been obtained in the range of 510–650 nm. A poor reflectance response, over most part of the visible spectrum, gives rise to a strong absorption feature and, consequently, a black appearance. In contrast, while the green wing specimen offered a uniform reflectance (~13%) over the aforesaid range, the coloured wing exhibited a steady rising trend, between 13 and 16%. At an orientation of 45° and 90° of the incident light, the reflectance was seen to be adequately lowered as witnessed in the green and multi-coloured wings. The details can be found at <https://iopscience.iop.org/article/10.1209/0295-5075/119/66003>

#### b) Whitish structural colouration in butterfly wings across *Lepidoptera* order

After a close inspection of the butterfly wings of white admiral (WA, *Limenitis Camilla*), large white (LW, *Pieris Brassicae*) and dark blue tiger (DBT, *Tirumala Septentrionis*) family, one could notice a dull, non-sticky feature in the first kind. The second kind gave a shiny lustre along with a noticeable white powdery substance, which would come off easily on touch. To be mentioned, the *Pierid* butterflies essentially possess pterin pigments which chiefly accounts for their whitish appearance [1,8]. Among different kinds of pterin, viz., leucopterin, erythropterin and xanthopterin, the white scales of *Pierids* are believed to contain leucopterin pigments [9]. Since the LW wing-type belongs to the *Pierid* family, it was believed to have evolved with sufficient pigmentary constituents. The WA and DBT butterfly wings, however, have no powdery substance, indicating that the striking white colouration is chiefly due to their specific built-in microstructures.

Earlier Siddique et. al. have examined the iridescent blue colouration in *Hypolimnna Salmacis* wings, and assigned the origin of blue colour to the stacking of black and brown scales [10]. In *Morpho Menelaus* wings, the angle modified discolouration effect was believed to have caused by adequate variation in optical thicknesses through chitin and air gaps [11]. We have also emphasized reflectance characteristics of the wing parts in responses to the variation in the wavelength and incident angles. Apparently, the specimens recorded a higher reflective feature at higher wavelengths and corresponding to a finite incident angle. In reference to the noticeable band maxima located at ~509 nm, as for the WA wing part, a growing reflectance trend has been witnessed with an increasing angle of incidence. When the incident angle is changed from 15° to 75°, the reflectance curves shoot up gradually over the whole spectral region. Earlier, as for the LW butterfly wing, a broadband reflectance with a higher reflectivity feature was noted over the visible and NIR regions. The reflectance, particularly, in the visible region is independent of the angle of incidence. The variation in reflectance curves with incident angle as displayed by the DBT specimen was in between the responses that of WA and LW wing parts. The condition for constructive interference relevant to thin layers is [12],

$$2d (n_2 - n_1/n_2^2) = m\lambda \cos\theta,$$

$$\text{with } \cos\theta = \sqrt{1 - \left(\frac{n_1}{n_2}\right)^2 \sin^2\phi}$$

Here,  $\phi$  is the angle of incidence,  $\theta$  is the diffraction angle in the medium,  $\lambda$  is the wavelength maxima and  $m$  ( $=1$ ) is the order of diffraction. The refractive indices of air and chitin material that make up the wings are respectively,  $n_1=1$  and  $n_2=1.56$  [13]. Considering 509 nm peak maxima under normal incidence ( $\phi = 0$ ,  $\theta = 0$ ), the optical path length as estimated for the WA butterfly wing,  $d=276.9$  nm. Similarly, the DBT wing specimen that exhibited reflectance peak maxima at 450 nm, gives  $d=245.9$  nm. Moreover, with a varying angle of incidence, we anticipate a profound alteration in optical paths ( $d \pm \Delta d$ ), which would affect the scattering effects profoundly.

c) Unusually diverse surface wettability in butterfly wings across *Lepidoptera* order

The microstructure-led dewetting features of the three distinct butterflies belonging to the *Lepidoptera* order have been discussed in the light of experimental data and representative models: Cassie-Cassie (C-C), Cassie-Wenzel (C-W), Wenzel-Cassie (W-C), Wenzel-Wenzel (W-W) and Vertical Gibbosity (V-G) based one. Although the wing scales varied with regard to the intra-scale geometrical constructs, the average width of the scales ranged between 46–56  $\mu\text{m}$ , while the separation between the longitudinal ridges measures approximately, 2.75  $\mu\text{m}$ . The DBT wing specimen contained two kinds of scales, short and large ones, the latter being more periodic and closely packed. Amongst all the wing types, the LW wing specimen offers a contact angle (CA) of  $\sim 100^\circ$ , indicating a smooth surface structure. This is because, the wing part is covered with adequate pterin pigments, which help fill the voids and air gaps prevailing in the scale microstructure.

Earlier Fang *et al.* have hypothesized three generic models based on the wing scale structures, which comprise of regular vertical gibbosities (V-G) with finite dimensions [14,15]. While the first proposition emphasizes the micro-class roughness which arises due to regularly arranged flat scales, the second model is based on the sub-micron class roughness and thus depends on the presence of vertical gibbosities. Finally, the third model prescribes the effective CA,  $\theta_t$  owing to the combinatorial effect of both micro-class and sub-micron class contributions to wettability and formulated in conformity with the aforesaid C-W model as,

$$\cos \theta_t = \varphi_t (r_t \cos \theta + 1) - 1,$$

in which,  $\varphi_t = \frac{bf}{ce}$

and  $r_t = \sqrt{\frac{4d^2}{f^2} + 1}$ .

Here, effective surface roughness ( $r_t$ ) is the ratio between the actual area to the projected area of independent vertical gibbosities of the triangular cross-section. Apparently,  $\frac{bf}{ce}$  is the effective water-solid fraction, recognizing the symbols  $b$ ,  $c$ ,  $d$ ,  $e$  and  $f$  as the average width of the scale, the distance between the consecutive scales, height of the vertical gibbosity, distance between any two gibbosities and width of each gibbosity; respectively. Recognizing  $\varphi_t = \varphi_m \varphi'_m = bf/ce$  and  $r_t = r_m$ , we can also introduce micro-roughness,  $r_m$  given by,

$$r_m = \sqrt{1 + \frac{b^2}{4a^2}}.$$

Using microscopic parameters in the respective equations, CA values were estimated theoretically and compared with those acquired through experimental means. Interestingly,  $r_m$  value is close to unity in all the cases, though one would appreciate higher  $r_m$  values attributed to sub-micron/nanoscale roughness.

As compared to the other wing types, the CA hysteresis ( $=17.5^\circ$ ) was quite low in the case of the LW wing surface. It is worth mentioning here that, the WA and DBT wings were believed to rely on sub-micron class surface roughness mediated dewetting features and are in conformity with the V-G as well as, C-W and V-G based models. Both the WA and DBT wings exhibited static CAs  $> 120^\circ$ , and that, the latter wing-part owing to a relatively lower surface adhesion could not hold the liquid droplet beyond a base-tilting angle of  $50^\circ$ . The wettability was seen to be greatly influenced by the wing surface microtexture, with a maximal roughness factor of 1.7. The detailed description about model validation on surface wettability of wings is located at, <https://iopscience.iop.org/article/10.1088/1402-4896/abe82e/meta>

#### d) Surface wettability and colouration/dicolouration response of *Indian Rosaceae*

Essentially, white (W), light pink (LP) and dark pink (DP) rose petals have been studied in detail. The petal surfaces are essentially hydrophobic with a maximum water CA exhibited by the DP specimen. Two well-accepted models are generally used to describe wetting-dewetting phenomena: Cassie-Baxter (C-B) and Wenzel models [16,17]. In fact, surface roughness and chemical composition both play dominant roles for displaying hydrophobicity [18]. On the other hand, the CA hysteresis is an important feature in examining (high or low) surface adhesion to water especially for hydrophobic surfaces [19]. In this regard, the petal effect is considered a surface phenomenon that is characterized by a large CA, CA hysteresis and strong adhesion to water. Different rose varieties can have petals with both high and low surface adhesion. In reality, for a surface with microstructure/nanostructure make-up (e.g., assembly of micro-papillae in rose petals), water can slowly adsorb into the pockets of the air gaps, resulting in a continuous transition from de-wetting to wetting feature [20].

The physical parameters that would help in determining wetting and de-wetting characteristics are: pitch value ( $p$ ), diameter ( $d$ ) and pitch-base height ( $h$ ). The pitch value is defined as the average peak-to-peak distance between any two micro-papillae, whereas, pitch-base height represents the approximate height of the micro-papillae. A smaller value of  $p/h$  ratio applies to the C-B regime, which tends to increase the static water CA. This ratio is important in the sense that, a lower value enhances the formation of air pockets between the microstructures, and consequently, the water droplet cannot come in contact with the bottom surface [20]. For a surface with prevailing micro and nanoscale roughnesses, the hydrophobic response will be affected by both of these while it is difficult to isolate individual contributions. For simplicity, the approximate microstructure roughness factor ( $r_s$ ) can be calculated by visualizing the micro-papillae as regular cylinders characterized by diameter ( $d$ ), height ( $h$ ) and pitch value ( $p$ ) that can be found over a square area. The roughness factor,  $r_s$  can be defined as the ratio of the actual, effective surface area to the projected, geometrical surface area. In a square area of length equal to the pitch value, the projected surface area is,  $p^2$ ; whereas the actual area is the sum of the curved surface area of the cylinder and the exposed surface area. The actual surface area is,  $p^2 + \pi dh$ . For the cylinder with the top being in contact with the water droplet [21],

$$r_s = 1 + \frac{\pi dh}{p^2} .$$

And the fraction of the solid-liquid contact under the droplet that would participate in the wetting-de-wetting mechanism can be expressed as,

$$\varphi = \frac{\pi d^2}{4p^2} .$$

Combining the above two expressions, one can interrelate surface roughness with the fractional solid-liquid contribution through the equation,

$$\varphi = \frac{d}{4h} (r_s - 1)$$

The aforesaid parameters along with the CA of petals are enlisted in Table 1.

As can be noticed, the DP rose exhibited the highest water CA, roughness factor and a low  $p/h$  ratio. The  $r_s$  value as high as, 3.21 and a  $\varphi$  value of 0.48 have been realized in this case. Among all the specimen types, the off pink, LP rose petals showed lower values of  $r_s$  and  $\varphi$ . It is apparent that a higher value of the roughness factor is likely to improve the solid-water fraction and consequently, hydrophobicity. Improved surface roughness and CA are mainly responsible for displaying dewetting feature of the DP rose petal. On the other hand, the water droplet may develop a tendency to impregnate into the grooves for a less rough surface. A different correlation account between  $r_s$  vs.  $\varphi$  has been found for damsel and dragonfly wings in one of our earlier work [22].



**Table 1:** Measured parameters related to dewetting phenomena witnessed in rose-petal surfaces

Sample	Bump density (1/10,000 $\mu\text{m}^2$ )	Static CA (deg.)	Roughness factor, $r_s$	Solid-water fraction, $\varphi$	Advancing and receding CA (deg.)	Transitional roughness, $r_t$	CAH (deg.)	Critical angles, $\alpha_1$ ; $\alpha_2$ (deg.)	Surface energy (mJ/m <sup>2</sup> )
White rose, W	27	122.5±0.2	2.74	0.37	137; 86	1.23	51±0.31	18°; –	49.8
Light pink rose, LP	33	111.2±0.2	2.27	0.32	117;90	1.83	27±0.27	29°; 57°	152.8; 264
Dark pink rose, DP	24	133.3±0.2	2.94	0.46	142;83	1.15	59±0.33	18°; 39°	13.1; 28.6

In order to examine the effect of structural and pigmentary contributions, the rose petals were adequately dipped in ethanol for quite some time. The idea behind ethanolic adsorption was to alter the micro-morphological features by varying the RI of the environment, which could bring in significant changes in the reflectance spectra. Earlier, the appearance of colour was believed to be caused by the change in the RI of the building elements or through transient modification in its dimensions [23]. The ethanol-soaked petals gave distinctly different characteristics with the appearance or smearing out of peak for a given specimen type. Whereas, a marginal peak shifting was observable for the LP rose petal, the DP specimen offered the emergence of a new peak located at ~465 nm. After ethanolic treatment, the LP rose petal gave a shifting of the peak from the value of ~455 nm to 480 nm in the reflectance spectra. The reflectance spectra for the white petals, before and after ethanolic treatment, however, were largely consistent throughout all wavelengths, but with smearing out of the broad peak in the case of the treated specimen. Moreover, upon comparing the spectral feature of the treated petals, one could realize a great similarity in the reflectance responses exhibited by the LP and DP petals. The relationship between optical stop-bands and the periodicity of a nano-structured system can be given by Bragg's law [24]:

$$\lambda = 2d n_{\text{eff}},$$

$$\lambda' = 2d n_{\text{eff}}' = 2d (n_{\text{eff}} + \Delta n) = 2d n_{\text{eff}} \left[ 1 + \frac{\Delta n}{n_{\text{eff}}} \right],$$

where  $n_{\text{eff}}$  is the effective RI of the system under study and  $d$  is the period that is assumed to be unaltered before and after ethanol adsorption. The RI of the air gaps, rose to contain geraniol, and ethanol is respectively 1.0, 1.46 and 1.36. Consequently,  $n_{\text{eff}}$  will be 1.23 and 1.27 for the untreated and ethanol treated cases knowing that many ultra-small air pockets will remain unfilled. Inserting  $\lambda=455$  nm and  $n_{\text{eff}}=1.23$  in the above eqn., we obtain  $d \sim 185$  nm. Apparently, this cannot be compared to the pitch of the micro-papillae which has a micron-scale dimension. However, the periodicity could be linked to the average repeat units of the nano-folders and air gaps that make up the micro-papillae. On substituting the values,  $d \sim 185$  nm and  $n_{\text{eff}} = 1.27$ , we obtained  $\lambda' = 472$ , which is close to the shifted peak position ( $\lambda' = 480$  nm). This slight departure can be ascribed to the relatively lowered sharing of the air gaps, as compared to geraniol and ethanol. The peak at a higher wavelength for the rose petals could indicate colour that results in a mutual combination of structure and pigment [24].

At the microstructure level, both the LP and DP rose petals share a common texture after the ethanol insertion. Accordingly, similar reflectance responses and chromaticity features have been observed. This is, because, ethanol may cover up many of the rough surfaces by way of filling air pockets/voids available within and around the micro-papillae. The visible light would experience adequate surface scattering from the bumpy assembly of micro-papillae which greatly depends on varying  $p/h$  value. Moreover, a lowered bump density and pitch value in the DP petals offered a stronger absorption feature and consequently, a deep

pink appearance to the unaided eye. For details, one may visit the following link- <https://link.springer.com/article/10.1007/s42235-018-0089-6>

## Conclusions

- Manifested spectral features have been observed due to the incorporation of Ag<sup>+</sup> into uni-coloured (black: *Papilio Liomedon*; light green: *Catopsilia Pyranthe*) and multi-coloured (*Vanessa Cardui*) butterfly wing scales. The light green and multi-coloured wings were found to be more sensitive to the orientation of the *p*-polarized light about the plane of incidence as compared to their black wing counterpart. The time-dependent progressive uptake of Ag<sup>+</sup> into the ridges of the wing scales has been confirmed through the EDX analyses and characterizes an exponentially growing trend ( $\sim e^{0.36t}$ ) for both uni- and multi-coloured wings.

-The origin of whitish structural colouration has been encountered in the white-appearing parts of the three important butterflies (WA, LW and DBT) belonging to the *Lepidoptera* order. In the LW case, the whitish colour is viewing angle independent as witnessed from its weak dependency of the reflectance response with the incident angle variation ( $\theta_i=15-75^\circ$ ). The thin-film interference augmented by coherent sub-surface scattering is anticipated particularly, in the whitish WA and DBT wing-types, whereas, the LW wing primarily gets its whiteness via non-absorbing leucopterin pigments. Polarisation-sensitive reflectance studies have revealed that, DBT is less sensitive to polarization as compared to the WA and LW wings.

- With CAs in the range of  $100^\circ-124^\circ$ , the WA, LW and DBT butterfly wings exhibit distinctly different surface wettability owing to their unique microstructural constructs of scales with the built-in ridges and cross-ribs. Generic models predict a roughness factor close to 2, where as CA hysteresis would alter in the range,  $17.5^\circ-45.7^\circ$ . A droplet kept on the DBT wing was seen to roll off the surface when the base was tilted with the horizontal plane, above  $50^\circ$ . The WA wing surface wettability was believed to closely obey the C-W model, while the DBT wing part supported the W-C and V-G based models, to a great extent.

-The wettability of rose (*Indian rosaceae*) and hibiscus (*Rosa sinensis*) flower petals were found to be largely dependent on their micro-papillae assembly and nanofolders therein. With a lowered pitch-to-height ratio, the DP rose petals recorded a very high static CA ( $= 133^\circ$ ),  $r_\phi = 2.94$  and CAH =  $59^\circ$  as compared to their W and LP counterparts. Consequently, the DP specimen was close to its superhydrophobicity criterion (CA $>140^\circ$ ). The reflectance features of the LP and DP specimens after ethanol treatment are quite similar owing to the establishment of a common surface structure. Similarly, propanol treatment gave quite alike reflectance features, for all the cultivar types. The dimension and distribution of the micro-papillae or micro-bumps, were believed to influence the surface morphology profoundly. In the case of the dry hibiscus petals, the reflectance declines owing to the buckling of micro-papillae and nanofolders being devoid of water.

## Scope of future works

There is a lot to explore in the upcoming field, called softonics that would profoundly connect concepts of soft-matter physics with optical and photonics principles. The attributes of biophotonic colouration, and dewetting features found in floral parts, plants, insects, avians and aquatic species draw the natural attention of the bystanders since the human civilization began its journey on our planet. The quest for knowing structure, colour, property and perception of living and non-living matter has been the key to scientific knowledge. Thus understanding the origin of structural colour and affinity to water in the aforesaid systems would strengthen our insight on morphogenesis and evolutionary mechanism at large. Naturally occurring photonic structures with the inclusion of metallic nanoparticles need more investigations to ensure nanophotonics and plasmonics on a complementary role for intended applications. The viewing

angle dependency, polarization sensitivity, and their modulation effects would help to visualize artificial designs, coatings, and camouflage in specific applications.

Through bio-mimicking and replication, one can also translate the structure-property relationship to structures developed through artificial means [25-28]. Possible fabrication of the intended structures with bi-functional properties has implications in numerous technological assets and products. To name a few are, smart window panels, screens, paints, textiles, etc. which may ensure perfect self-cleaning as well as color matching, as per requirement. On the other hand, the moth-eye structure is known to be the most advanced field of biomimicry due to its low reflection response in a wide range of wavelengths and angles of incidence. Nanoimprint lithography is the frequently applied technique for fabricating such structures. Similarly, artificial superhydrophobic surfaces are fabricated mimicking rose-petal and lotus effects. There are also recent reports of fabrication of self-cleaning polymer by mimicking leaf microstructures. These directions need to be strengthened further to warrant proof-of-principle concepts.

To be mentioned, the validation of Wenzel, Cassie-Baxter and similar models has not been encountered for textured surfaces of different species emphasizing advantages and limitations. Attempts may be given to model contributions arising due to micro and nanoscale roughnesses in the system of interest. Moreover, special efforts may be extended to find model systems available in nature for optical transparency, anti-reflecting property, iridescent colouration, concealing colouration as well as superhydrophobicity.

## References

1. B. Wijnen, H.L. Leertouwer, D.G. Stavenga, *J. Insect Physiol.* **53**, 1206 (2007).
2. G.A.Cordell, *The Alkaloids: Chemistry and Biology*; 1<sup>st</sup> edition, Academic Press: San Diego (2003).
3. R.Boruah, P. Nath, D.Mohanta, G.A.Ahmed, A.Choudhury, *Nanosci. Nanotechnol. Lett.* **3**, 458 (2011).
4. P. Vukusic, J. R.Samples, *Nature* **424**, 852 (2003).
5. <sup>a)</sup> S.Kinoshita, *Structural colour in the realm of nature*, World Scientific, Singapore (2008); <sup>b)</sup> S. Kinoshita Biophotonics-An Introductory Text Book, Pan-Stanford Publishing Ltd., Singapore (2013).
6. P.R.Stoddart, P.J. Cadusch, T.M. Boyce, R.M. Erasmus, J.D. Comins, *Nanotechnology* **17**, 680 (2006).
7. G. Waldman, *Introduction to light : the physics of light, vision, and colour*, Dover Press (2002).
8. B. D. Wilts, B. Wijnen, H. L. Leertouwer, U. Steiner, D. G. Stavenga, *Adv. Opt. Mater.* **5**, 1600879 (2017).
9. D. G. Stavenga, H. L. Leertouwer and B. D. Wilts, *J. Exp. Biol.* **217**, 2171 (2014).
10. R. H. Siddique, S. Vignolini, C. Bartels, I. Wacker and H. Hölscher, *Sci. Rep.* **6**, Art.No.36204 (2016).
11. S.C. Niu, B. Li, J. F. Ye, *Sci. China Tech. Sci.* **59**, 749 (2016).
12. J.H. Simmons and K.S. Potter, *Optical Materials* (Academic Press, 2006) pp.184.
13. O. Deparis, C. Vandembem, M. Rassart, V. L. Welch, J.-P. Vigneron, *Opt. Exp.* **14**, 3547 (2006).
14. Y. Fang, G. Sun, T. Wang, Q. Cong and L. Ren, *Chin. Sci. Bull.* **52**, 711-716 (2007).
15. Y. Fang, G. Sun, Y. Bi and H. Zhi, *Sci. Bull.* **60**, 256-63 (2015).
16. A. B. D Cassie. *Discus. Faraday Soc.*, **3**, 11 (1948).
17. R.N. Wenzel, *J. Phys. Chem.* **53**, 1466 (1949).
18. R. Blossey, *Nat. Mater.* **2**, 301 (2003).
19. B. Bhushan, M. Nosonovsky, *Philos. Trans. Roy. Soc. A*, **368**, 4713 (2010).
20. A. J. Schulte, D.M. Droste, K. Koch, W. Barthlott, *Beilstein J. Nanotechnol.* **2**, 228 (2011).
21. E. Bormashenko, T. Stein, R. Pogreb, D. Aurbach, *J. Phys. Chem. C*, **113**, 5568 (2009).
22. S.N.Aideo, D.Mohanta, *Appl. Surf. Sci.* **387**, 609 (2016).

23. H.M. Whitney, M. Kolle, P. Andrew, L. Chittka, U. Steiner, B.J. Glover, *Science*, **323**, 130 (2009).
24. L. Feng, Y. Zhang, M. Li, Y. Zheng, W. Shen, L. Jiang, *Langmuir*, **26**, 14885 (2010).
25. A. Saito, *Sci. Technol. Adv. Mater.* **12**, 064709 (2011).
26. O. Deparis, S. Mouchet, L. Dellieu, J. F. Colomer and M. Sarrazin, *Mater. Today: Proceedings* **1**, 122 (2014).
27. S. Zhang, J. Huang, Z. Chen, and Y. Lai, *Small*, **13**, 1602992 (2017).
28. T. Darmanin, F. Guittard, *Mater. Today*, **18**, 273 (2015).
29. D. Helmer, N. Keller, F. Kotz, C. Greiner, T. M. Narang, K. Sachsenheimer, B.E. Rapp, *Sci. Rep.* **7**, Art.No. 15078 (2017).

\*\*\*

## UTILISATION CERTIFICATE

(FOR THE FINANCIAL YEAR ENDING 31<sup>st</sup> March 2021)

UC pertains to

First release	Second release	Third release	Fourth release	Final release
---------------	----------------	---------------	----------------	---------------

Is the UC provisional?: **Provisional, Annual**

1. Title of the Project/Scheme: **Studies on bifunctional (wetting-dewetting and biophotonic colouration) properties of certain natural systems of biological origin**
2. Name of Principal Investigator: **Dr. Dambarudhar Mohanta**
3. Implementing Institution: **Tezpur University**
4. SERB sanction order no. and date: SERB/F/4981/2017-2018 dated 17 Aug.2017  
SERB/F/11476/2018-2019 dated 22 Feb. 2019  
SERB/F/8441/2019-2020 dated 02 January 2020
5. Amount brought forward from the : **Rs. 2,21,039/-**  
previous financial year quoting SERB letter number and date in which the authority to carry forward the said amount was given:
6. a) Amount received during the financial year (Please give SERB letter/order no. and date for the amount) : **NIL**  
b) Interest earned, if any: **Rs. 1,136/-**
7. Total amount that was available for expenditure (excluding commitments) during the financial year (Sr. No. 5+6a+6b): **Rs. 2,22,175/-**
8. Actual expenditure (excluding commitments) incurred during financial year (upto 31<sup>st</sup> March 2021): **Rs. 1,75,607/-**
9. Balance amount available at the end of the: **Rs. 46,568/-**  
financial year (8-9):  
OR  
Negative balance (If the expenditure incurred is: **NA**  
more than the funds released)
10. Unspent balance if any refunded to SERB: **Rs.46,568/-**  
(give details of cheque/DD no.)
11. Amount to be carried forward to the next: **NIL (Project completed)**  
financial year (if any):

UTILISATION CERTIFICATE

12. Certified that out of Rs. NIL of Recurring grants- in –aid sanctioned during the year 2020-21 in favour of the Registrar, Tezpur University under SERB letter/order No. SERB/F/4981/2017-2018 dated 17 Aug.2017, SERB/F/11476/2018-2019 dated 22 Feb. 2019, SERB/F/8441/2019-2020 dated 02 Jan. 2020 and Rs. 2,21,039/- on account of unspent balance of the previous year and Rs.1,136/- earned through interest, a sum of Rs. 1,75,607/- has been utilized for the purpose for which it was sanctioned and that the balance of Rs. 46,568/- remaining unutilized until the completion of the project and being sent to SERB by electronic transfer/<sup>dd</sup>mode.

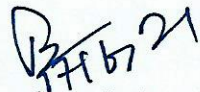
Certified that we have satisfied ourselves that the conditions on which the grants-in-aid were sanctioned have been fulfilled/are being fulfilled and that we have exercised the following checks to see that the money was actually utilised for the purpose for which it was sanctioned.

Kinds of checked exercise

- 1.
- 2.

  
Signature of PI

  
Signature of Registrar/Account officer

  
Signature of Head of Institution

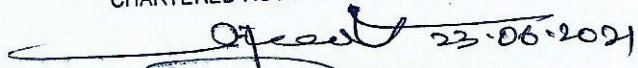
Date Investigator  
Principal  
DST-SERB/IAC/CSIR Project  
Department of Physics  
Tezpur University

Date: Finance Officer  
Tezpur University

Date: Registrar  
Tezpur University

Science and Engineering Board

For SURAJIT CHAKRABORTY & CO.  
CHARTERED ACCOUNTANTS

  
CA, SURAJIT CHAKRABORTY  
(Proprietor)  
Membership No.- 305054

UC has been accepted by

Signature:

Name of the SERB officer:

Designation:

A/c Page only

SESHAASA(AIC) / CTS-2010

भारतीय स्टेट बैंक  
State Bank of India  
Issuing Branch: TEZPUR UNIVERSITY  
कोड नं. / CODE No: 14259  
Tel No. 03712-267285

मांगद्राफ्ट  
DEMAND DRAFT

Key: WIFLES  
Sr. No: 754360

2 1 0 6 2 0 2 1  
D D M M Y Y Y Y

मांगे जानेपर FUND FOR SCIENCE & ENGINEERING RESEARCH\*\*\*\*\*

या उनके आदेश पर

ON DEMAND PAY

OR ORDER

रुपये RUPEES

Forty Six Thousand Five Hundred and Sixty Eight Only

अदा करें

₹

46568.00

IOI 000471535180  
Name of Applicant

Key: WIFLES Sr. No: 754360  
TEZPUR UNIVERSITY R&D

AMOUNT BELOW 46569(0/5)

मूल्य प्राप्त / VALUE RECEIVED



भारतीय स्टेट बैंक

STATE BANK OF INDIA

अदाकर्ता शाखा / DRAWEE BRANCH: NEW DELHI MAIN BRANCH

कोड नं. / CODE No: 00691

प्राधिकृत हस्ताक्षरकर्ता  
AUTHORISED SIGNATORY

शाखा प्रबंधक  
BRANCH MANAGER

*Satyajit Mazumdar*

₹ 1,50,000/- एवं अधिक के लिखत दो अधिकारियों द्वारा हस्ताक्षरित होने पर ही वैध है।  
INSTRUMENTS FOR ₹ 1,50,000/- & ABOVE ARE NOT VALID UNLESS SIGNED BY TWO OFFICERS

कम्प्यूटर द्वारा मुद्रित होने पर ही वैध  
VALID ONLY IF COMPUTER PRINTED

केवल 3 महीने के लिए वैध  
VALID FOR 3 MONTHS ONLY

⑈ 535180⑈ 000002000⑈ 000471⑈ 16

सत्यजीत मजूमदार  
SATYAJIT MAZUMDAR  
M 13712

9  
6  
5  
4  
3  
2  
1

## UTILISATION CERTIFICATE

(FOR THE FINANCIAL YEAR ENDING 31<sup>st</sup> March 2021)

UC pertains to

First release	Second release	Third release	Fourth release	Final release
---------------	----------------	---------------	----------------	---------------

Is the UC provisional?: **Provisional, Annual**

1. Title of the Project/Scheme: **Studies on bifunctional (wetting-dewetting and biophotonic colouration) properties of certain natural systems of biological origin**
2. Name of Principal Investigator: **Dr. Dambarudhar Mohanta**
3. Implementing Institution: **Tezpur University**
4. SERB sanction order no. and date: SERB/F/4981/2017-2018 dated 17 Aug.2017  
SERB/F/11476/2018-2019 dated 22 Feb. 2019  
SERB/F/8441/2019-2020 dated 02 January 2020
5. Amount brought forward from the : **NIL**  
previous financial year quoting SERB letter number and date in which the authority to carry forward the said amount was given:
6. a) Amount received during the financial year: **NIL**  
(Please give SERB letter/order no. and date for the amount):  
b) Interest earned, if any: **NA**
7. Total amount that was available for expenditure (excluding commitments) during the financial year (Sr. No. 5+6a+6b): **NIL**
8. Actual expenditure (excluding commitments) incurred during financial year (upto 31<sup>st</sup> March 2021): **NIL**
9. Balance amount available at the end of the: **NIL**  
financial year (8-9):  
OR  
Negative balance (If the expenditure incurred is: **NA** more than the funds released)
10. Unspent balance if any refunded to SERB: **NIL**  
(give details of cheque/DD no.)
11. Amount to be carried forward to the next financial year (if any): **NIL (Project completed)**




UTILISATION CERTIFICATE


12. Certified that out of Rs. 0 /-of Non-Recurring grants- in –aid sanctioned during the year 2020-21 in favour of the Registrar, Tezpur University under SERB letter/order No. SERB/F/4981/2017-2018 dated 17 Aug.2017, SERB/F/11476/2018-2019 dated 22 Feb. 2019 SERB/F/8441/2019-2020 dated 02 Jan. 2020 and NA on account of unspent balance of the previous year, a sum of NIL has been utilised for the purpose for which it was sanctioned and that the balance of Rs. 0 /- remaining unutilised at the end of the financial year 2020-21.

Certified that we have satisfied ourselves that the conditions on which the grants-in-aid was sanctioned have been fulfilled/are being fulfilled and that we have exercised the following checks to see that the money was actually utilised for the purpose for which it was sanctioned.

Kinds of checked exercise

- 1.
- 2.

  
Signature of PI

Date:   
Principal Investigator  
DST-SERB/IUGC/SIR Project  
Department of Physics  
Tezpur University

Signature of Registrar/Account officer

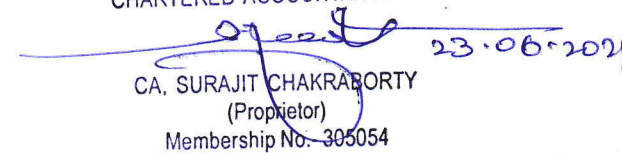
Date:   
Finance Officer  
Tezpur University

Signature of Head of Institution

Date: Registrar  
Tezpur University

Science and Engineering Board

For SURAJIT CHAKRABORTY & CO.  
CHARTERED ACCOUNTANTS

  
CA. SURAJIT CHAKRABORTY  
(Proprietor)  
Membership No. 305054

23.06.2021

UC has been accepted by

Signature:

Name of the SERB officer:

Designation:

**REQUEST FOR ANNUAL INSTALMENT WITH UP-TO-DATE STATEMENT OF EXPENDITURE**

1. SERB Sanction Order No and date: **EMR/2016/008045 and SERB/F/4981/2017-2018 dated 17 August 2017**
2. Name of the PI: **Dr. Dambarudhar Mohanta**
3. Total Project Cost: **Rs. 43,66,560/-**
4. Revised Project Cost: (if applicable)
5. Date of Commencement: **17.11.2017**
6. Statement of Expenditure: **Please see column-7 below**

Month and year	Expenditure incurred/committed

Grant received in each year:

- a. 1st Year: **Rs. 28, 50, 000/-**
- b. 2nd Year: **Rs. 4,00,000/-**
- c. 3rd Year: **Rs. 5,00,000/-**
- d. 4<sup>th</sup> year:
- e. Interest, if any: **Rs. 1,136/-**
- f. Total (a + b + c + d + e): **37,51,136/-**

## Statement of Expenditure

7. (For financial year 17.11.2017 till 16.11.2020)

Sl No (I)	Sanctioned Heads (II)	Total Funds Allocated (indicate sanctioned or revised (III))	Total Funds received (IV)	Fund received (2017-18) (V)	Fund received (2018-19) (VI)	Fund received (2019-20) (VII)	Fund received (2020-21) (VIII)	Expenditure Incurred				Total Expenditure (XIII = IX + X+XI+XII)	Balance as on date (XIV = IV - XIII)
								1 <sup>st</sup> yr (IX)	2 <sup>nd</sup> yr (X)	3 <sup>rd</sup> Year (XI)	4 <sup>th</sup> Year (XII)		
1	Manpower costs							65,419	1,78,903	1,78,968	1,04,258	5,27,548	
2	Consumables							40,634	NIL	41,060	47,685	1,29,379	
3	Travel	14,69,600	8,53,040	2,17,680	3,08,000	3,27,360	NIL	NIL	23,543	NIL	NIL	23,543	33,528
4	Contingencies							52,449	13,022	49,907	23,664	1,39,042	
5	Others, if any (Interest)		1,136				1,136	NIL	NIL	NIL	NIL	NIL	1,136
6	Equipment	25,00,000	25,00,000	25,00,000	0	0	NIL	NIL	25,00,000	NIL	NIL	25,00,000	NIL
7	Overhead expenses	3,96,960	3,96,960	1,32,320	92,000	1,72,640	NIL	1,12,346	93,142*	1,79,568	0	3,85,056	11,904
8	Total	43,66,560	37,51,136	28,50,000	4,00,000	5,00,000	1,136	2,70,848	28,08,610	4,49,503	1,75,607	37,04,568	46,568

\*The extra amount of Rs.46,207/- spent against equipment is adjusted from the Overhead expenses.

\*\*The unspent amount of Rs. 46,568/- being sent through electronic transfer/ dd mode.

Name and signature of Principal Investigator  
Date:

*(P. Mohanty)*  
Principal Investigator  
DST-SERB/AAAG/CSIR-Project  
Department of Physics  
Tezpur University

Signature of competent financial authority (with seal)  
Date:

*(Finance Officer)*  
Tezpur University

For SURAJIT CHAKRABORTY & CO.  
CHARTERED ACCOUNTANTS

*(Proprietor)*  
CA. SURAJIT CHAKRABORTY  
Membership No./ 305054